COMPDYN 2015
5th ECCOMAS Thematic Conference on
Computational Methods in Structural Dynamics and Earthquake Engineering
M. Papadrakakis, V. Papadopoulos, V. Plevris (eds.)
Crete Island, Greece, 25–27 May 2015

SIMPLIFIED SEISMIC COLLAPSE ASSESSMENT OF GENERIC FRAME STRUCTURES SUBJECTED TO PDELTA AND MATERIAL DETERIORATION

David Kampenhuber[1] **and Christoph Adam**[2]

[1] Unit of Applied Mechanics, University of Innsbruck, Innsbruck, Austria
e-mail: david.kampenhuber@uibk.ac.at

[2] Unit of Applied Mechanics, University of Innsbruck, Innsbruck, Austria
e-mail: christoph.adam@uibk.ac.at

Keywords: Generic frame structures, material deterioration, PDelta effect, seismic excitation, simplified collapse assessment

Abstract. *In this paper the influence of material deterioration on the seismic collapse capacity of PDelta vulnerable frame structures is quantified. The main objective is to reveal and to validate the range of applicability of the proposed equivalent single-degree-of-freedom (ESDOF) system for assessment of the global collapse capacity. This is achieved through comparison of the median collapse capacity of PDelta vulnerable generic frame structures that exhibit material deterioration in strength and stiffness with outcomes of the corresponding ESDOF system based on the derived transformation rules. Sets of planar generic frame structures are compiled varying the governing structural parameters for seismic collapse independently. In all cases, the collapse capacity is calculated using incremental dynamic analysis. Record-to-record variability of the collapse capacity is studied using a set of ordinary earthquake records compiled in FEMA-P695.*

1 INTRODUCTION

For professionals in engineering practice it is desirable to have simplified methods for the seismic assessment of structures available. An example is the response spectrum method, where the effect of inelastic structural behavior and overstrength is considered via a reduction of the pseudo-acceleration demand leaving the seismic analysis completely elastic. In a more recent development the collapse capacity spectrum method [4] aims at assessing the seismic collapse capacity of highly inelastic PDelta vulnerable frame structures without conducting nonlinear time history analysis. The main assumptions of the latter method are that the impact of material deterioration on seismic sidesway collapse of moment resisting frame structures is negligible compared to the destabilizing effect of gravity loads, and that collapse is governed by the fundamental mode. The application of all of these methods requires the engineer to examining carefully the underlying assumptions and restrictions for the considered structure to be assessed. Based on the modified Ibarra-Medina-Krawinkler deterioration model [14], Kampenhuber, Adam [17] quantified the effect of material deterioration on the collapse capacity of PDelta vulnerable single-degree-of-freedom (SDOF) systems considering different material deterioration modes. As a result, for SDOF systems exhibiting nonlinear cyclic behavior sets of parameter combinations have been identified, where PDelta, material deterioration, or a combination of both effects simultaneously governs seismic collapse. To include this knowledge into the framework of the collapse capacity spectrum methodology, Kampenhuber, Adam [16] proposed a procedure how the deterioration parameters of the modified Ibarra-Medina-Krawinkler model [14] assigned to the nonlinear components of a frame structure can be transformed into the domain of the corresponding equivalent SDOF (ESDOF) system. Based on regression analyses, the present contribution describes an enhanced version of the transformation rules for these material parameters. A validation is provided for a set of generic planar multi-degree-of-freedom (MDOF) frame structures subjected to the 44 ordinary earthquake records of FEMA-P695 report [11]. Incremental dynamic analysis (IDA) up to collapse is conducted both for each frame structure and the corresponding ESDOF model, and the resulting median collapse capacities are set in contrast. The results presented here aim at assessing the accuracy and the range of applicability of the proposed simplified collapse prediction procedure. Note that in this contribution the expression "deterioration" only refers to the successive reduction of material/component quantities such as strength and unloading stiffness as a result of cyclic deformation. The degrading effect of PDelta on the structure is not addressed with this expression. Moreover, superscript $(\cdot^{wG})$ refers to quantities considering gravity loads (read: "with gravity"), whereas superscript $(\cdot^{woG})$ represents parameters disregarding gravity loads (read: "without gravity").

2 GENERIC FRAME STRUCTURES AND STRUCTURAL MODELING STRATEGY

The investigated multi-story frame structures are based on the ones presented in Medina, Krawinkler [22], which have already been used in other studies such as in Ibarra, Medina, Krawinkler [14], Lignos, Krawinkler [19], Jäger [15], and Adam, Jäger [4]. These n story generic moment-resisting single-bay frame structures of uniform story height h, designed according to the weak beam-strong column design philosophy, are composed of rigid beams, elastic flexible columns, and inelastic rotational springs at the beam ends and the base according to a concentrated plasticity formulation. To each joint of the frames an identical point mass $m_i/2 = m_s/2$, $i = 1, \ldots, n$, and an identical gravity load is assigned. Figure 1 shows exemplarily a four-story frame.

The targeted straight-line fundamental mode shape is the governing condition for adjusting

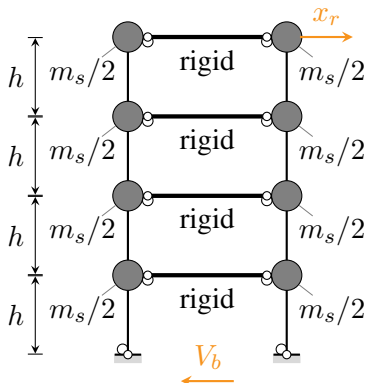

Figure 1: Mechanical model of e. g. a four-story MDOF system.

the bending stiffness of the columns and the initial stiffness of the springs. Coefficient τ relates the fundamental period without gravity loads, T_1^{woG}, and the number of stories of the frame structures, n,

$$T_1^{woG} = \tau n \tag{1}$$

and thus, quantifies the global lateral stiffness of the structure. According to Ibarra, Medina, Krawinkler [14], periods $T_1^{woG} = 0.10n$ and $T_1^{woG} = 0.20n$ are a reasonable lower and upper bound for moment-resisting frames, representing stiff and flexible structures, respectively.

The strength of the rotational springs is tuned with the result that in a first mode pushover analysis without taking into account gravity loads yielding is initiated at all springs simultaneously. A predefined base shear coefficient γ of 0.10, i. e. the base shear without gravity loads at the onset of yielding $V_{b,y}^{woG}$ over the total structural weight $W = Mg$, $M = \sum_{i=1}^{n} m_s$, governs the magnitude of the yield strength [22]. To the rotational springs a bilinear backbone curve is assigned. That is, a linear elastic branch of deformation is followed by a linear inelastic branch with reduced stiffness, characterized by the strain hardening coefficient α_s, which is the same for all springs of the considered MDOF models: $\alpha_s = 0.03$.

The hysteretic response of the springs is assumed to be bilinear. Deterioration of the bilinear hysteretic cyclic behavior is simulated with the modified Ibarra-Medina-Krawinkler deterioration model [13]. This bilinear constitutive model exhibits unloading stiffness deterioration and cyclic strength deterioration, controlled by deterioration parameters Λ_K and Λ_S, respectively. The further deterioration modes *accelerated reloading stiffness deterioration* and *post-capping strength deterioration*, which may be captured by the modified Ibarra-Medina-Krawinkler deterioration model, do not apply in this case. For details it is referred to [14, 13, 19]. For the sake of simplicity, unloading stiffness deterioration and cyclic strength deterioration parameters Λ_K and Λ_S, respectively, are assumed to be equal, $\Lambda_S = \Lambda_K$. To all springs of a frame the same deterioration parameters Λ_K and Λ_S are assigned. Lignos, Krawinkler [19, 18] compiled a database of experimental cyclic studies on steel components, which allowed to identify the significant parameters affecting the cyclic moment-rotation relationship at plastic hinge regions in beams. Based on this study, in the present publication three different levels of deterioration, representing slow, medium, and rapid deterioration, have been defined.

The PDelta effect on the frame structures is quantified by two base shear-roof drift (V_b–x_r) relations (referred to as global pushover curves) resulting from two different first mode pushover analyses [4]. In one pushover analysis the constant gravity loads are applied to the model, whereas the second pushover analysis is conducted without gravity loads. For the present

generic frame structures both global pushover curves are bilinear, because at all springs yielding is initiated simultaneously. As depicted in Figure 2, the PDelta effect leads for a given roof displacement to a reduction of the base shear, and thus, to an apparent reduction of the lateral stiffness.

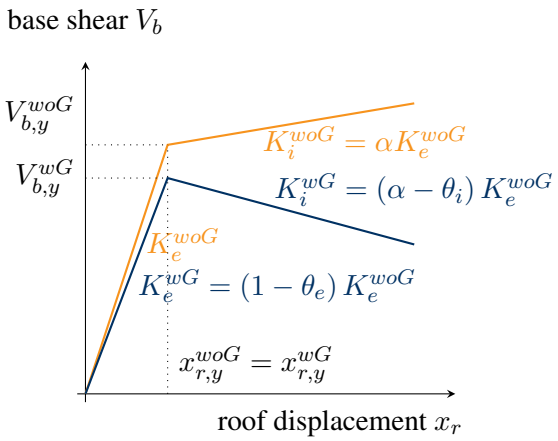

Figure 2: Global pushover curves of MDOF system considering and disregarding gravity loads

It has already been shown by Medina, Krawinkler [22] that for multi-story frame structures this stiffness reduction is different in the elastic and inelastic deformation branch of the global pushover curve. Consequently, additionally to the lateral global hardening coefficient α, an elastic and an inelastic stability coefficient, θ_e and θ_i, respectively, which characterize the magnitude of the stiffness reduction in these branches, can be identified from the pushover curves,

$$\theta_e = 1 - \frac{K_e^{wG}}{K_e^{woG}} \quad , \quad \theta_i = \alpha - \frac{K_i^{wG}}{K_e^{woG}} \tag{2}$$

Note that in general the lateral global hardening coefficient α is not the same as the strain hardening coefficient α_s assigned to each rotational spring.

In the present study the difference $\theta_i - \alpha$, i. e. the normalized slope of the inelastic deformation branch (also referred to as negative post-yield stiffness ratio), is the target variable that characterizes the PDelta effect on the frame structure (compare with Figure 2) [6]. Thus, for each structure with different properties but the same $\theta_i - \alpha$ value, the ratio ν of total gravity load over dead weight is in general different. This is a contrast to previous studies of the authors [17, 15, 6], where the PDelta effect was characterized by a constant gravity load coefficient ν.

Rayleigh type damping enforcing $5\,\%$ viscous damping of the first mode and of the mode, where $95\,\%$ of the total mass is included, is considered. The corresponding damping matrix is proportional to the mass matrix and the current stiffness matrix.

All predefined basic model parameters of the considered generic frame structures are summarized in Table 1.

3 EQUIVALENT SINGLE-DEGREE-OF-FREEDOM SYSTEM

If the response is dominated by the first mode of vibration, it is reasonable to assume that an ESDOF system captures the global seismic response. This is in general the case for low- to medium-rise regular planar frame structures up to nine stories. However, Adam, Jäger [4] have shown that an ESDOF system even can be used to estimate the seismic collapse capacity of high-rise frame structures if collapse is primarily governed by PDelta.

Table 1: Summary of basic model parameters of the considered frame structures

Variable	Description	Range of values
n	Number of stories	1 to 20
τ	Global stiffness quantification factor	$0.10, 0.12, 0.14, 0.16, 0.18, 0.20$
$\Lambda_K = \Lambda_S$	Deterioration parameter representing slow, medium and rapid deterioration, respectively	$2.0, 1.0, 0.5$
α_s	Strain hardening coefficient of rotational springs	0.03
$\theta_i - \alpha$	Negative post-yield stiffness ratio	$0.03, 0.04, 0.05, 0.06, 0.10, 0.20, 0.30, 0.40$
γ	Base shear coefficient at yield	0.10

The basic assumption of most ESDOF models is that the vertical distribution of the horizontal deformations of the MDOF structures does not change during the cyclic excitation. That is, the deflected shape remains constant throughout the time history regardless of the amount of inelastic deformations. This assumption can be expressed as

$$\mathbf{x} = \boldsymbol{\psi} x_r \tag{3}$$

where $\mathbf{x}$ is the displacement vector of the story masses, x_r denotes the roof displacement, and $\boldsymbol{\psi}$ is a time independent shape vector, which describes the horizontal displacement pattern according to a fundamental mode approximation. Consequently, if the real behavior of the MDOF differs significantly from this assumption, an ESDOF system will be in general less appropriate for predicting the seismic collapse capacity.

In this section it is described how the parameters of a generic frame structure can be transformed into the domain of the corresponding ESDOF system, based on a shape vector that is identical with the first mode: $\boldsymbol{\psi} = \boldsymbol{\phi}_1$. With increasing complexity of the MDOF model this transformation becomes more and more tricky. In particular, when strength and stiffness of the components deteriorate, additional considerations are required that are not treated in the literature yet.

Subsequently, parameters with a superscript $(\cdot^*)$ represent quantities of the ESDOF system. The ESDOF model and the underlying MDOF model used in this study is sketched in Figure 3. It is characterized by a rigid, massless rod of length h^* with a lumped mass L^* [2, 8, 9],

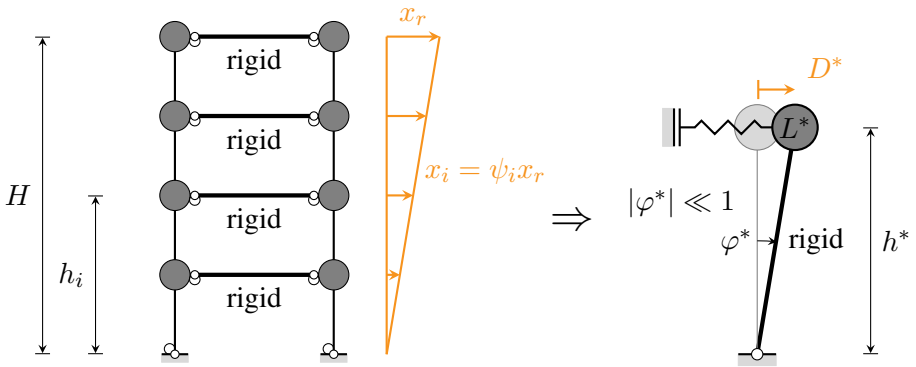

Figure 3: Utilized equivalent single-degree-of-freedom model

$$h^* = \frac{\sum_{i=1}^{n} h_i m_i \phi_{1,i}}{\sum_{i=1}^{n} m_i \phi_{1,i}} = \frac{\sum_{i=1}^{n} h_i \phi_{1,i}}{\sum_{i=1}^{n} \phi_{1,i}} \quad , \quad L^* = \sum_{i=1}^{n} m_i \phi_{1,i} = m_s \sum_{i=1}^{n} \phi_{1,i} \tag{4}$$

at its tip, and a horizontal translational spring attached to the lumped mass with assigned nonlinear material properties. In equation (4) h_i represents the height of the ith story with respect to the base (see Figure 3), and $\phi_{1,i}$ is the ith element of shape vector $\boldsymbol{\phi_1}$. In accordance with Chopra [8], h^* represents the first mode modal height h_1^* and L^* the modal mass of the first mode of vibration of the MDOF model. It is recalled that equation (4) simplifies because the mass matrix of the considered generic frames is diagonal with equal mass coefficients $m_s = m_i$ for each story i.

According to Adam, Krawinkler [5] earthquake induced collapse is sufficiently accurate represented by small displacement theory, and thus, the geometric linearized horizontal tip displacement $D^* = \varphi^* h^*$ serves as engineering demand parameter (EDP). Defining equilibrium on the deformed shape, vertical forces (i. e. gravity loads) affect the horizontal displacement, referred to as PDelta effect. Note that the post-buckling behavior of the considered model is equivalent to an inverted mathematical pendulum with a rotational spring at its base (as used in Adam, Krawinkler [5]) because small displacement theory is employed [10].

The backbone curve of the ESDOF system is based on the base shear-roof drift relations from a first mode pushover analysis, as shown in orange color in Figure 2. Accordingly, yield strength $f_y^{*,woG}$, yield displacement D_y^*, elastic stiffness $K_e^{*,woG}$, and period $T^{*,woG}$ of the ESDOF model without gravity loads reads as [4]

$$f_y^{*,woG} = \frac{V_{b,y}^{woG}}{\Gamma^*} \quad , \quad D_y^* = \frac{x_{r,y}}{\Gamma^*} \quad , \quad K_e^{*,woG} = \frac{f_y^{*,woG}}{D_y^*} \quad , \quad T^{*,woG} = 2\pi \sqrt{\frac{L^*}{K_e^{*,woG}}} \tag{5}$$

$V_{b,y}^{woG}$ represents the base shear, and $x_{r,y}$ the roof displacement at the onset of yielding of the MDOF model subjected to a first mode pushover analysis, and Γ^* is the effective participation factor,

$$\Gamma^* = \frac{L^*}{m^*} \quad , \quad m^* = \sum_{i=1}^{n} m_i \phi_{1,i}^2 = m_s \sum_{i=1}^{n} \phi_{1,i}^2 \tag{6}$$

3.1 Incorporation of the PDelta effect into the ESDOF system

In the present study the PDelta effect is incorporated into the ESDOF system depicted in Figure 3 as proposed by Adam, Ibarra, Krawinkler [2] and Ibarra, Krawinkler [13]. Basis of quantification of PDelta are the global pushover curves from first mode pushover analyses with and without considering gravity loads as shown in Figure 4.

Since in a real SDOF system PDelta is governed by a single stability coefficient [21], the bilinear pushover curves of the MDOF model, however, exhibit an elastic and an inelastic stability coefficient [22], Ibarra, Krawinkler [13] derived an auxiliary ESDOF system with a uniform (auxiliary) stability coefficient $\theta^{*,a}$. $\theta^{*,a}$ is a function of θ_e, θ_i and α^* [13],

$$\theta^{*,a} = \frac{\theta_i - \theta_e \alpha^*}{1 - \theta_e + \theta_i - \alpha^*} \tag{7}$$

Stiffness $K_e^{*,a,woG}$, and the yield strength $f_y^{*,a,woG}$ of this auxiliary ESDOF system is derived from the corresponding parameters of the ESDOF system that is not affected by PDelta [2, 13],

$$K_e^{*,a,woG} = \frac{1 - \theta_e + \theta_i - \alpha^*}{1 - \alpha^*} K_e^{*,woG} \qquad f_y^{*,a,woG} = \frac{1 - \theta_e + \theta_i - \alpha^*}{1 - \alpha^*} f_y^{*,woG} \tag{8}$$

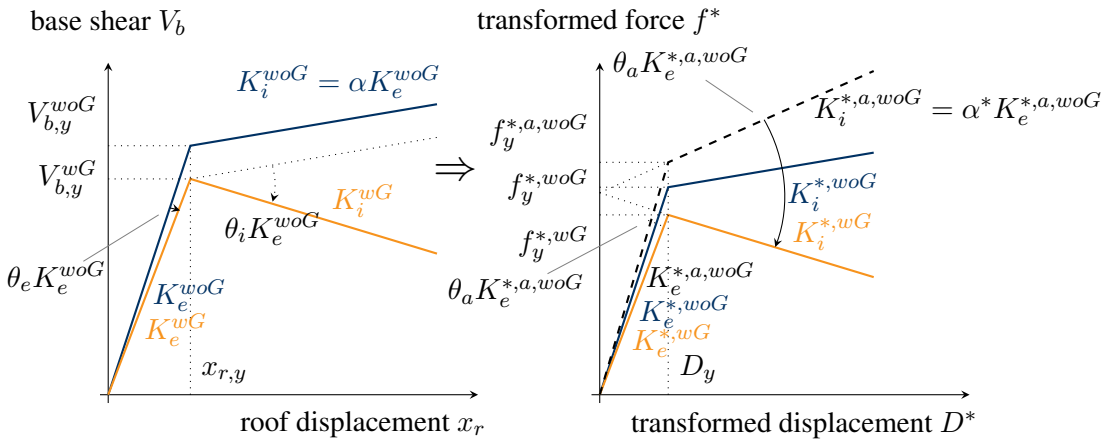

Figure 4: Transformation of global pushover curves of the MDOF model (left subplot) into the domain of the ESDOF system. Right subplot: backbone curve of the auxiliary ESDOF system (black graph), and of the ESDOF system considering gravity loads (orange graph) .

For the period $T^{*,a,woG}$ of the auxiliary ESDOF system the following relation holds:

$$T^{*,a,woG} = T^{*,woG}\sqrt{\frac{1-\alpha^*}{1-\theta_e+\theta_i-\alpha^*}} \tag{9}$$

To simulate the PDelta effect, this auxiliary ESDOF system with stiffness $K_e^{*,a,woG}$ is loaded by the gravity load $P^{*,a}$, which is related to the auxiliary stability coefficient $\theta^{*,a}$ according to MacRae [21]

$$P^{*,a} = \theta^{*,a} K_e^{*,a,woG} h^* \tag{10}$$

The right subplot of Figure 4 shows in black the backbone curve of the auxiliary ESDOF system, and in orange of the ESDOF system considering gravity loads. The blue graph refers to the transformed pushover curve disregarding gravity loads.

3.2 Transformation of the deterioration parameters into the ESDOF domain

Based on cyclic pushover analyses and subsequent optimization analyses [7, 12], Kampenhuber, Adam [16] identified in a previous study a relation between the component deterioration parameters Λ_K and Λ_S assigned to the rotational springs of the considered generic frame structures and the corresponding parameters Λ_K^* and Λ_S^* of the ESDOF system. The resulting median deterioration parameter ratios Λ_K^*/Λ_K and Λ_S^*/Λ_S are depicted in Figure 5 by markers.

It is readily observed that these ratios become larger with increasing period $T^{*,a,woG}$ and stiffness quantification coefficient τ. The full lines represent the corresponding regression curves, which can be expressed as a function of $T^{*,a,woG}$ as follows:

$$\Lambda_m^*/\Lambda_m = a\left(T^{*,a,woG}\right)^b + c \quad , \quad m = K, S \tag{11}$$

Coefficients a, b, and c listed in Table 2 are different for unloading stiffness (Λ_K^*) and cyclic deterioration (Λ_S^*), and depend on the global stiffness coefficient τ of the MDOF system.

With given stiffness quantification coefficient τ of the MDOF model, $T^{*,a,woG}$, and coefficients a, b, c, the deterioration parameter ratio according to equation (11) can be evaluated.

In an analysis disregarding PDelta, the deterioration parameter should be read at the ESDOF model period $T^{*,woG}$. Subsequent multiplication of this ratio with the deterioration parameter

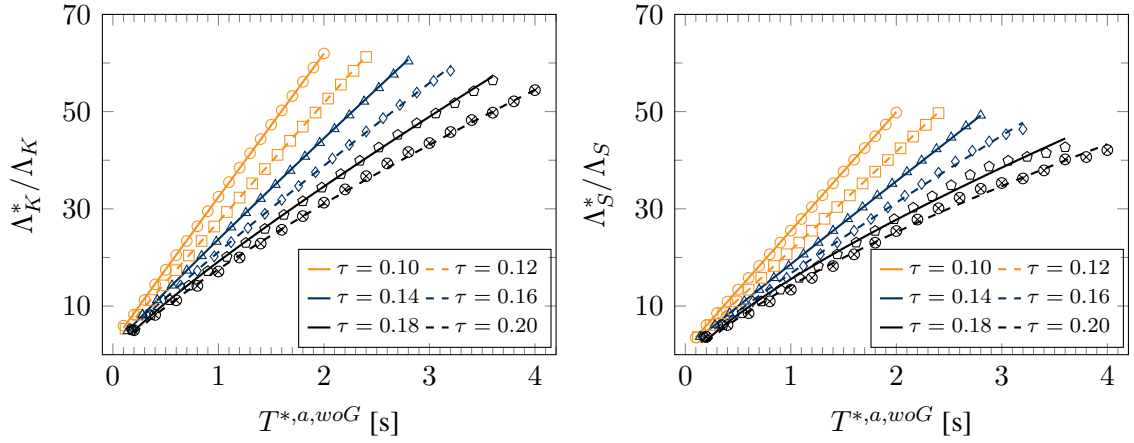

(a) (b)

Figure 5: Relation between deterioration parameters of the ESDOF and the MDOF model based on the period of the ESDOF model: median and regression curve

Table 2: Coefficients for evaluation of equation (11)

	$\tau = 0.10$			$\tau = 0.12$			$\tau = 0.14$		
	a	b	c	a	b	c	a	b	c
Λ_K^*/Λ_K	29.96	0.99	2.45	25.48	0.97	1.88	22.30	0.95	1.43
Λ_S^*/Λ_S	24.39	1.00	1.14	20.30	1.00	1.17	17.55	0.98	1.07
	$\tau = 0.16$			$\tau = 0.18$			$\tau = 0.20$		
	a	b	c	a	b	c	a	b	c
Λ_K^*/Λ_K	19.90	0.92	1.21	18.96	0.86	0.19	18.18	0.80	-0.62
Λ_S^*/Λ_S	16.79	0.90	-0.06	17.94	0.75	-2.41	16.99	0.72	-2.79

assigned to the rotational springs (Λ_K, Λ_S) in the frame structure renders the corresponding quantity ($\Lambda_K^{*,a}$, $\Lambda_S^{*,a}$) for the auxiliary ESDOF system.

4 COLLAPSE CAPACITY, GROUND MOTION SELECTION, AND GROUND MOTION SCALING

In the present study the global seismic collapse capacity of the MDOF frame structures and the corresponding ESDOF systems is determined performing incremental dynamic analyses (IDA) [25]. In an IDA nonlinear response history analyses are conducted repeatedly, increasing in each subsequent run the ground motion intensity. As an outcome an appropriate measure of the intensity of the earthquake record is plotted against the EDP. The analysis is stopped when the structure collapses. In this study collapse is assumed to be indicated when an incremental increase of the intensity leads to an unbounded structural response. The corresponding intensity of the ground motion record is referred to as global seismic collapse capacity. For details of seismic collapse assessment it is referred to Adam, Ibarra [1]

In this contribution in the MDOF domain the 5 % damped spectral pseudo-acceleration S_a at the fundamental structural period (considering gravity loads) T_1^{wG} normalized with respect to the base shear coefficient γ^{wG} (considering gravity loads) at yield and acceleration of gravity g

is used as characteristic relative intensity of an earthquake record [24],

$$IM = \frac{S_a(T_1^{wG}, \zeta = 5\%)}{g\gamma^{wG}} \quad , \quad \gamma^{wG} = \frac{V_{b,y}^{wG}}{W} \tag{12}$$

As discussed in Tsantaki [24] it is beneficial to utilize in this definition of the relative intensity the structural quantities affected by gravity. The relative collapse capacity is therefore given by

$$CC = IM|_{collapse} \tag{13}$$

Accordingly, the relative collapse capacity in the ESDOF domain reads as

$$CC^{ESDOF} = \left.\frac{S_a(T^{*,a,wG}, \zeta = 5\%)}{g\gamma^{*,a,wG}}\right|_{collapse} \quad , \quad \gamma^{*,a,wG} = \frac{f_y^{*,a,wG}}{L^* g} \tag{14}$$

When transformed into the domain of the MDOF structure,

$$CC^* = \frac{CC^{ESDOF}}{\lambda^{IM}} \tag{15}$$

CC^* is assumed to be a reasonable approximation of the collapse capacity CC. Transformation coefficient

$$\lambda^{IM} = \frac{L^{*2}}{Mm^*} \tag{16}$$

relates collapse capacity of the MDOF and the ESDOF domain [4].

To capture the inherent record-to-record variability of the collapse capacity, in this study the 44 ordinary ground motions compiled in the far-field set of the FEMA P-695 report [11] are used, and subsequently median and dispersion of the 44 corresponding collapse capacities of each structure are evaluated.

5 EXACT VERSUS SIMPLIFIED COLLAPSE ASSESSMENT

5.1 Non-deteriorating frame structures ("base case")

At first the global seismic collapse capacity of frame structure that exhibit a negative post-yield stiffness ratio but no material deterioration is discussed. These structure are referred to as "base case", because the corresponding collapse capacities are compared with the ones of material deteriorating structures. Some of the presented results can also be found in Jäger [15].

Figure 6 shows contour plots of the median collapse capacity of non-deteriorating frame structures vulnerable to PDelta as a function of the number of stories n and the negative post-yield stiffness ratio $\theta_i - \alpha$.

The left subplot corresponds to stiff frames with a stiffness quantification coefficient $\tau = 0.10$, and the right subplot refers to flexible frames with $\tau = 0.20$. It can be seen that structures with a large negative post-yield stiffness ratio, i. e. $\theta_i - \alpha = 0.20$ to 0.40, the median collapse capacity is almost constant independently of the number of stories and stiffness quantification coefficient τ. In contrast, with decreasing PDelta vulnerability, i. e. $\theta_i - \alpha$ in the range of 0.03 to 0.05, the median collapse capacity varies with the number of stories and the structural stiffness. It is also observed that the magnitude of the median collapse capacity becomes larger with increasing number of stories and flexibility, and thus, with increasing fundamental structural period, compare with equation (1).

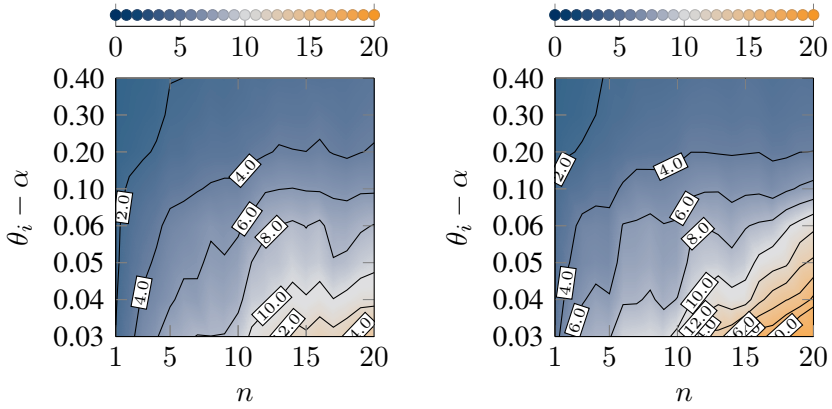

(a) $\tau = 0.10$; base case (b) $\tau = 0.20$; base case

Figure 6: Median collapse capacities (CC_{p50}) of non-deteriorating PDelta vulnerable frame structures (base case) for two stiffness quantification coefficients τ.

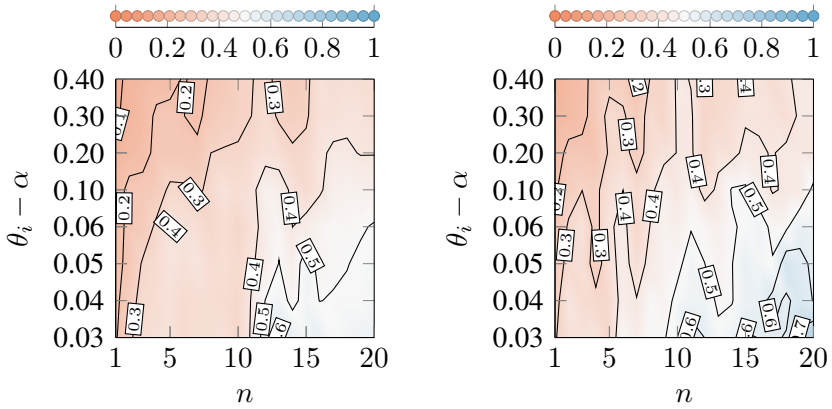

(a) $\tau = 0.10$; base case (b) $\tau = 0.20$; base case

Figure 7: Measure of dispersion (σ) of non-deteriorating PDelta vulnerable frame structures (base case) for two stiffness quantification coefficients τ.

For the same structural configurations, in Figure 7 the corresponding measure for the record-to-record dispersion $\sigma = \ln \sqrt{CC_{p84}/CC_{p16}}$ [20], where CC_{p84} and CC_{p16} denotes the 84th and 16th percentile, respectively, of the collapse capacity, is depicted. σ is a meaningful measure of dispersion because the record-to-record variability of the collapse capacity can be in general approximated by a log-normal distribution [23], confirmed in [4, 3] for PDelta sensitive structures. The outcomes show that σ is proportional to the building flexibility τ and the number of stories n, and it increases as τ and n increases. σ is inversely proportional to the vulnerability to PDelta expressed by $\theta_i - \alpha$, and it decreases as $\theta_i - \alpha$ increases. For instance, for a stiff one-story frame ($\tau = 0.10$, $n = 1$) highly vulnerable to PDelta ($\theta_i - \alpha = 0.40$), σ is 0.08. In contrast, a 20-story frame with the same negative post-yield stiffness ratio $\theta_i - \alpha = 0.40$ and the same stiffness quantification factor $\tau = 0.10$ the dispersion increases to $\sigma = 0.37$. For a very flexible ($\tau = 0.20$) 20-story highly structure highly vulnerable to PDelta ($\theta_i - \alpha = 0.40$), the dispersion becomes even larger, i. e. $\sigma = 0.42$. A slightly PDelta vulnerable flexible one-story building ($\theta_i - \alpha = 0.03$, $\tau = 0.20$, $n = 1$) exhibits the largest collapse capacity dispersion of $\sigma = 0.78$.

Each considered non-deteriorating MDOF structure is now transformed into the ESDOF domain according to the relations presented in section 3 for simplified collapse assessment. In an effort visualize domains, where the simplified predictions of the ESDOF system match the more time-consuming collapse predictions of the actual MDOF frame, in Figure 8 median collapse capacity ratios of the MDOF structure with respect to the ESDOF model, i. e. CC_{p50}/CC^*_{p50}, are plotted. A ratio of 1.0 implies that the "simplified" collapse capacity prediction based on

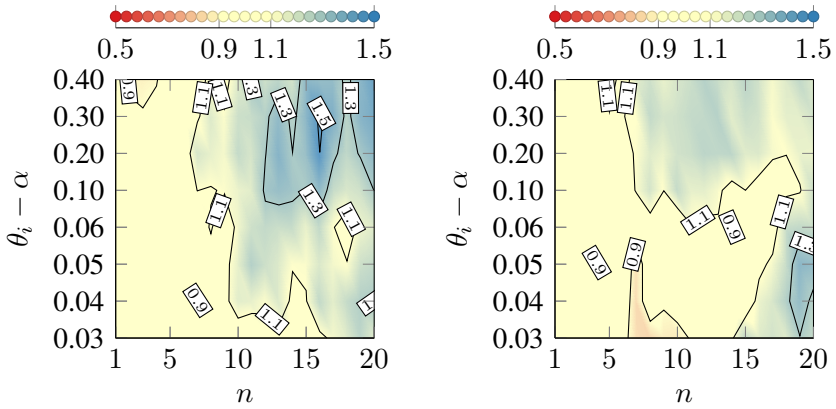

(a) $\tau = 0.10$; base case (b) $\tau = 0.20$; base case

Figure 8: "Exact" median collapse capacity over the median collapse capacity of the ESDOF system (CC_{p50}/CC^*_{p50}) of non-deteriorating frame structures (base case) for two stiffness quantification coefficients τ.

the ESDOF system coincides with the "exact" counterpart. If the median collapse capacity of the MDOF system is smaller than the median collapse capacity of the corresponding ESDOF model (i. e. $CC_{p50} < CC^*_{p50}$), the ratio is smaller than 1.0. In this figure the domain of $CC_{p50}/CC^*_{p50} < 0.90$ is plotted in red. Blue domains characterize those parameter configurations where the median collapse capacity of the MDOF structure is larger than the one of the ESDOF model: $CC_{p50} > CC^*_{p50}$.

The results of Figure 8a demonstrate that for stiff frame structures ($\tau = 0.10$) up to 10 stories the ESDOF system slightly overestimates the median collapse capacity by $10\,\%$ at most. With increasing number of stories ($n \geq 10$) and increasing negative post-yield stiffness ratio ($\theta_i - \alpha \geq 0.10$) the ESDOF system, however, underestimates this collapse quantity. For instance, for a 20-story stiff structure ($\tau = 0.10$) with $\theta_i - \alpha = 0.40$ the collapse capacity ratio CC_{p50}/CC^*_{p50} is 1.46. More flexible systems as shown in Figure 8b exhibit the same trend, however, in general the deviation between both predictions is smaller. From these results it can be concluded that global collapse of PDelta vulnerable frames up to 10 stories is primarily governed by the first mode, as it is assumed for simplified ESDOF system based collapse assessment.

5.2 Deteriorating frame structures

To assess the effect of material deterioration on the median collapse capacity of the considered frame structures, and in further consequence on the predictions based on the corresponding ESDOF systems, three different speeds of component deterioration are taken into account. As shown in Table 1 the deterioration speed effects the choice of the deterioration parameters Λ [13, 19].

In Figure 9 the derived median collapse capacities $CC^{deteriorating}_{p50}$ of these structures are

compared with the outcomes $CC_{p50}^{basecase}$ of the base case frames through representation of the collapse capacity ratios $CC_{p50}^{deteriorating}/CC_{p50}^{basecase}$. In the first row of Figure 9 (Figures 9a

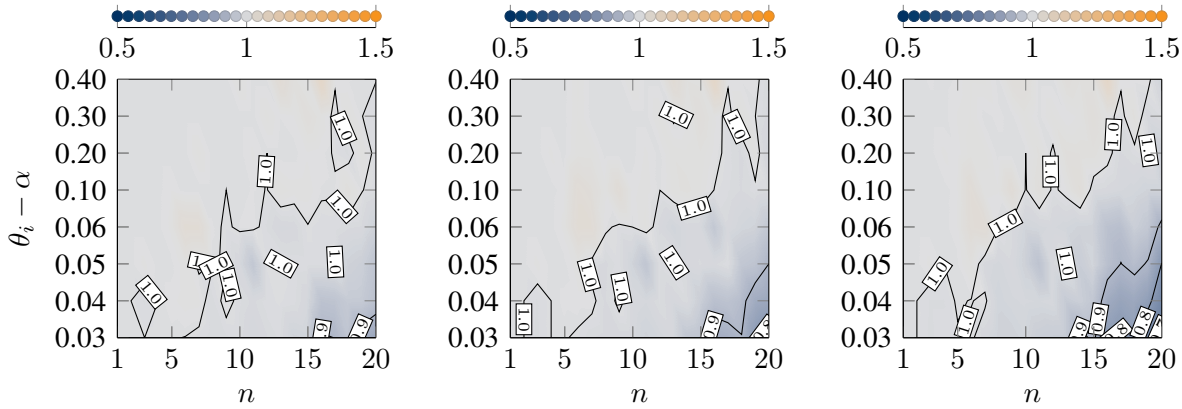

(a) $\tau = 0.10$; slow (b) $\tau = 0.10$; medium (c) $\tau = 0.10$; rapid

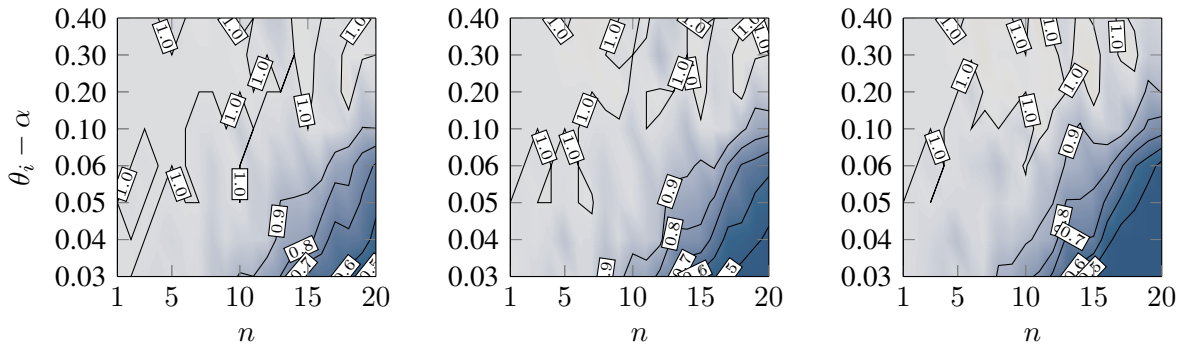

(d) $\tau = 0.20$; slow (e) $\tau = 0.20$; medium (f) $\tau = 0.20$; rapid

Figure 9: Median collapse capacity of deteriorating over the median collapse capacity of non-deteriorating frame structures ($CC_{p50}^{deteriorating}/CC_{p50}^{basecase}$) for two stiffness quantification coefficients τ and three "speeds" of component deterioration.

to 9c) the effect of three deterioration speeds on the collapse capacity ratios of *stiff* structures ($\tau = 0.10$) is visualized. It is readily observed that for the depicted structural domain the ratio is close to 1.0. That is, in these domains material deterioration does not affect significantly the median collapse capacity. Only for high-rise frames with small negative post-yield stiffness ratio $\theta_i - \alpha$ deterioration becomes more significant, in particular for rapid material deterioration. For instance, for a 20-story frame with $\theta_i - \alpha = 0.03$ the ratio $CC_{p50}^{deteriorating}/CC_{p50}^{basecase}$ is 0.68, which means that that material deterioration reduces the median collapse capacity by $32\,\%$. From these results it can be concluded that collapse of the considered stiff structures is primarily governed by PDelta.

The subplots of the second row of Figure 9 (Figures 9d to 9f) representing flexible frame structures ($\tau = 0.20$) show a different picture. It can be seen that material deterioration plays a more prominent role compared to stiff structures. For those *flexible* frames a significant influence of material deterioration on the median collapse capacity is observed if PDelta is less pronounced (i. e. $\theta_i - \alpha < 0.06$) and the number of stories is larger than 10. Here, the median collapse capacity ratio $CC_{p50}^{deteriorating}/CC_{p50}^{basecase}$ of the 20-story frame with $\theta_i - \alpha = 0.03$ is 0.23, which is about $66\,\%$ smaller than for the stiff counterpart structure.

Both stiff and flexible groups of frame structures have in common that the collapse capacity is only negligibly influenced by material deterioration if the structures are highly vulnerable to PDelta, i. e. the negative post-yield stiffness ratio $\theta_i - \alpha$ is larger than 0.20. Consequently, in this parameter domain the collapse capacity ratios shown in Figure 9 are close to 1.0.

In Figure 10 the measure of dispersion σ of the collapse capacity of the same group of material deteriorating PDelta vulnerable frame structures is depicted. The results of this figure

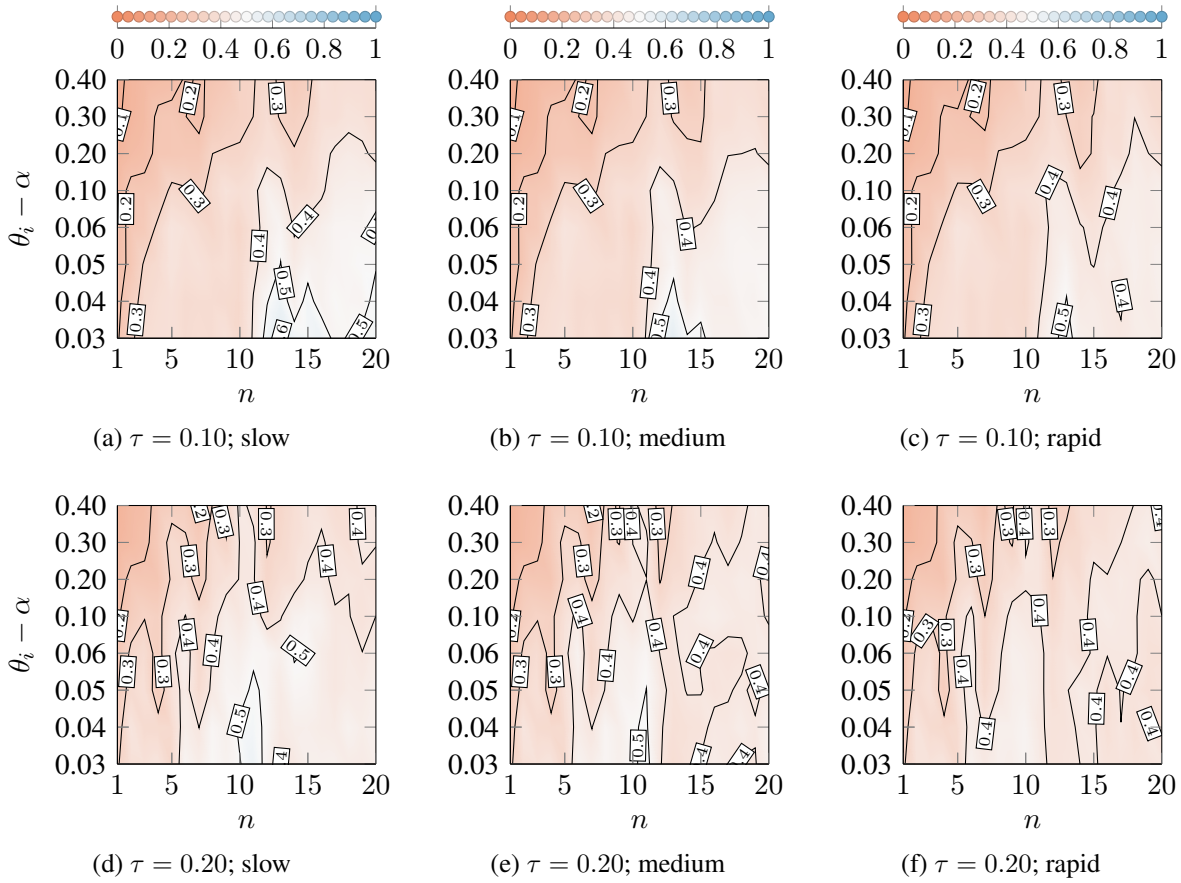

(a) $\tau = 0.10$; slow (b) $\tau = 0.10$; medium (c) $\tau = 0.10$; rapid

(d) $\tau = 0.20$; slow (e) $\tau = 0.20$; medium (f) $\tau = 0.20$; rapid

Figure 10: Measure of dispersion σ of deteriorating frame structures (corresponding to Figure 9) for two stiffness quantification coefficients τ and three "speeds" of deterioration.

reflect the trend of σ with respect to the number of stories and the negative post-yield stiffness ratios as observed for non-deteriorating structures, see Figure 7. Comparing the subplots of Figure 10 reveals that σ is not significantly affected by the deterioration speed. The difference between the outcomes of stiff and flexible structures is also small. For instance, for 10-story stiff deteriorating frames with $\theta_i - \alpha = 0.10$ dispersion measure σ is 0.36 for slow and medium deterioration and 0.37 for rapid deterioration. Flexible but otherwise frames with the same parameters exhibit a σ of 0.40 for slow, 0.39 for medium, and 0.41 for rapid deterioration. For these cases the corresponding dispersion ratios $\sigma^{deteriorating}/\sigma^{basecase}$ are close to 1.0, i. e. 1.006, 1.009, 1.042, 0.990, 0.967, and 1.018, respectively.

Next, simplified collapse capacity predictions based on the proposed ESDOF system, which captures also material deterioration, are evaluated. For each frame structure deterioration parameters have been calculated based on equation (11) and Table 2. The basic equivalent model parameters are defined as described in section 5.1. Figure 11 shows for the same structural

configurations as described before the ratio "exact" median collapse capacity CC_{p50} to the simplified prediction CC^*_{p50}: CC_{p50}/CC^*_{p50}. The yellow domain indicates ratios in the range of 0.9

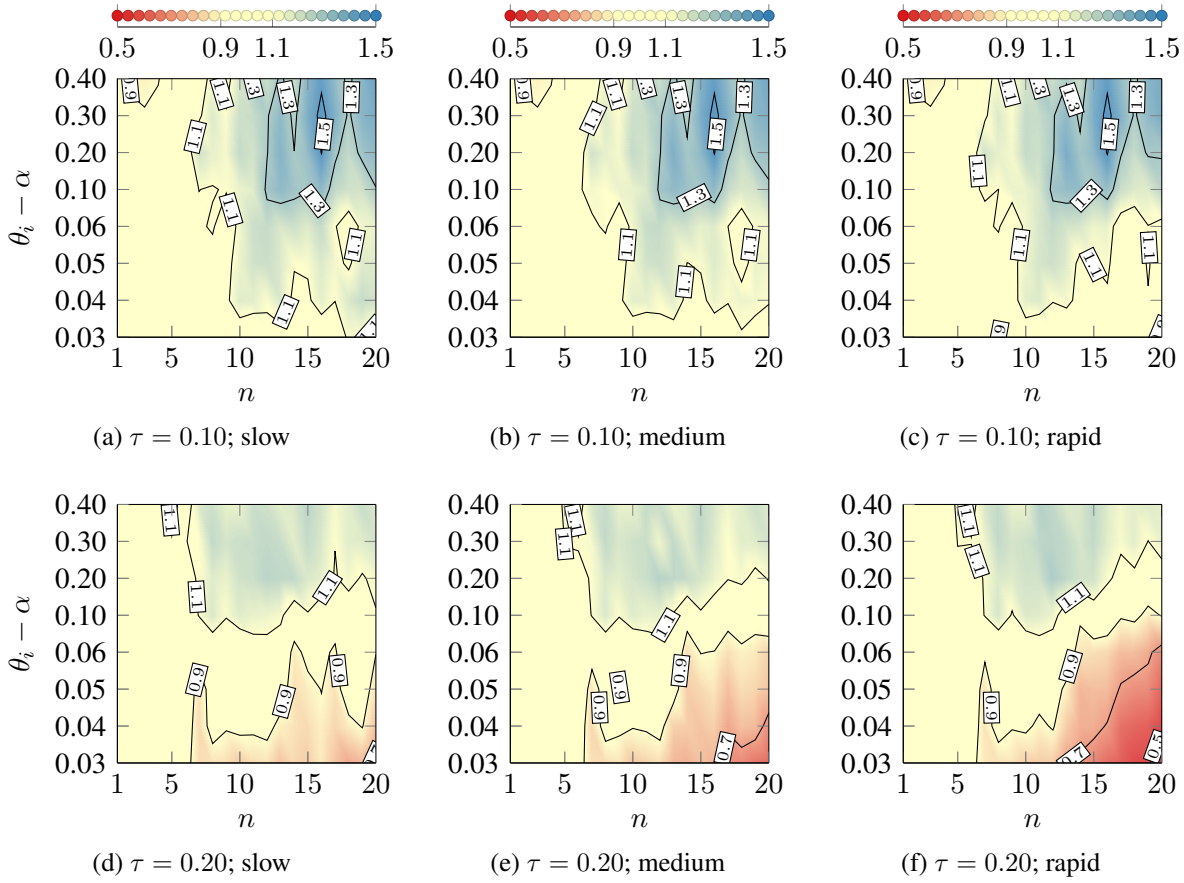

(a) $\tau = 0.10$; slow (b) $\tau = 0.10$; medium (c) $\tau = 0.10$; rapid

(d) $\tau = 0.20$; slow (e) $\tau = 0.20$; medium (f) $\tau = 0.20$; rapid

Figure 11: Deviation of the median collapse capacity of deteriorating frame structures based on an ESDOF model ($CC^{deteriorating}_{p50}/CC^{*,deteriorating}_{p50}$) for two stiffness quantification factor τ and three "speeds" of deterioration.

to 1.1. It can be seen that for frames up to 6 stories the median collapse capacity of the simplified model approximates the median collapse capacity of the MDOF model ($CC_{p50} \approx CC^*_{p50}$) within the accepted bounds. For a six-story structure the minimum ratio $CC_{p50}/CC^*_{p50}\Big|_{min}$ is 0.88 and the maximum one is 1.17. However, for stiff high-rise frames highly vulnerable to PDelta, the equivalent SDOF model underestimates the collapse capacity of the MDOF model, i. e. $CC_{p50}/CC^*_{p50} = 1.54$, or alternatively, $CC^*_{p50} = 0.65CC_{p50}$. This domain is depicted in blue. The results for stiff frames (Figures 11a to 11c) also reveal that the ESDOF system does not overestimate the median collapse capacity for any parameter combination. This holds, however, not true for flexible frames. Here the collapse capacity ratio becomes smaller than 1.0 if the negative post-yield ratio $\theta_i - \alpha$ is smaller than 0.06 and the number of stories exceeds 6. It is seen that the over-prediction of the collapse capacity increases with increasing deterioration speed. For instance, the extreme case is the 20-story frame with rapid deterioration and a negative post-yield stiffness ratio $\theta_i - \alpha = 0.03$, where the collapse capacity ratio CC_{p50}/CC^*_{p50} drops to a value of 0.47. That is an overestimation of the MDOF collapse capacity by a factor of about two.

5.3 Assessment of the proposed ESDOF model

The improvement of the simplified collapse assessment based on the novel deteriorating ESDOF model system compared to a non-deteriorating counterpart [4] is studied subsequently. Therefore, in Figure 12 the ratio of the exact median collapse capacity CC_{p50} of PDelta vulnerable "deteriorating" frame structures to the median collapse capacity of the corresponding "non-deteriorating" ESDOF model ($CC_{p50}^{*,basecase}$) is depicted. It is readily observed that the difference

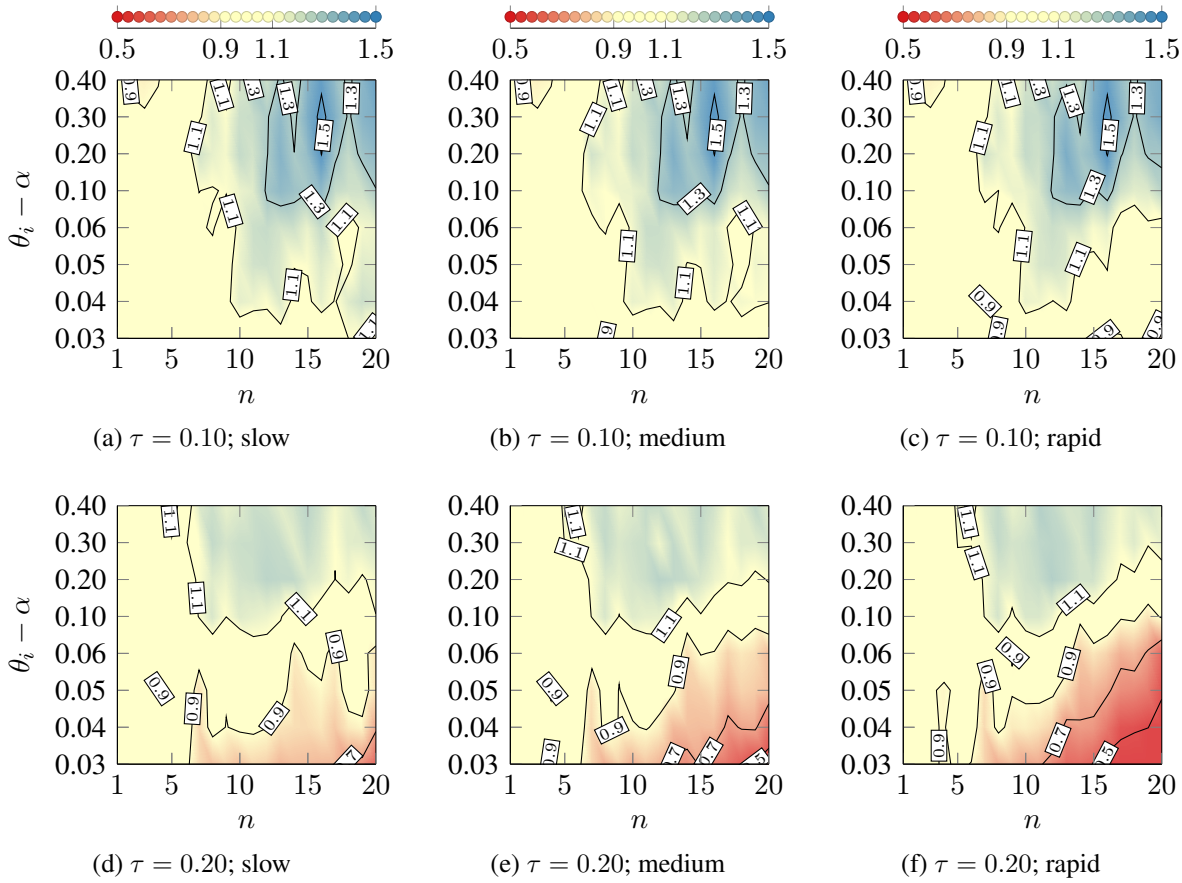

(a) $\tau = 0.10$; slow (b) $\tau = 0.10$; medium (c) $\tau = 0.10$; rapid

(d) $\tau = 0.20$; slow (e) $\tau = 0.20$; medium (f) $\tau = 0.20$; rapid

Figure 12: Efficiency of proposed ESDOF model for two stiffness quantification factor τ and three "speeds" of deterioration: median collapse capacity of deteriorating MDOF structure in relation to the outcome of non-deteriorating ESDOF system ($CC_{p50}^{deteriorating}/CC_{p50}^{*,basecase}$).

of Figure 12 and Figure 11 (non-deteriorating case) is comparatively small. In particular, when comparing the outcomes of the simplified assessment for stiff frame structures the results are of the same order. For instance, for a stiff 15-story building ($\tau = 0.10$) with $\theta_i - \alpha = 0.10$ the collapse capacity ratio is 1.31 for slow, 1.32 for medium, and 1.31 for rapid material deterioration. When using a non-deteriorating ESDOF system for the collapse assessment of a deteriorating frame structure, the accuracy of the collapse prediction decreases for high buildings that are less vulnerable to PDelta, in particular when they are flexible (Figures 12d to 12f). There the ratio $CC_{p50}/CC_{p50}^{*,basecase}$ is significantly smaller than 1.0 (highlighted in red color). In the extreme case of a 20-story rapid deteriorating frame structure with $\theta_i - \alpha = 0.03$, this ratio decreases to a minimum of 0.29, see Figure 12f. Thus, the collapse capacity of ESDOF model is 3.5 times larger than the "exact" one.

To visualize this loss of accuracy, the ratios of the ESDOF system based predictions without and with considering material deterioration, $CC_{p50}^{*,basecase}/CC_{p50}^{*,deterioration}$, are shown in Figure 13. It is observed that for PDelta vulnerable systems in the range $\theta_i - \alpha$ from 0.10 to 0.20

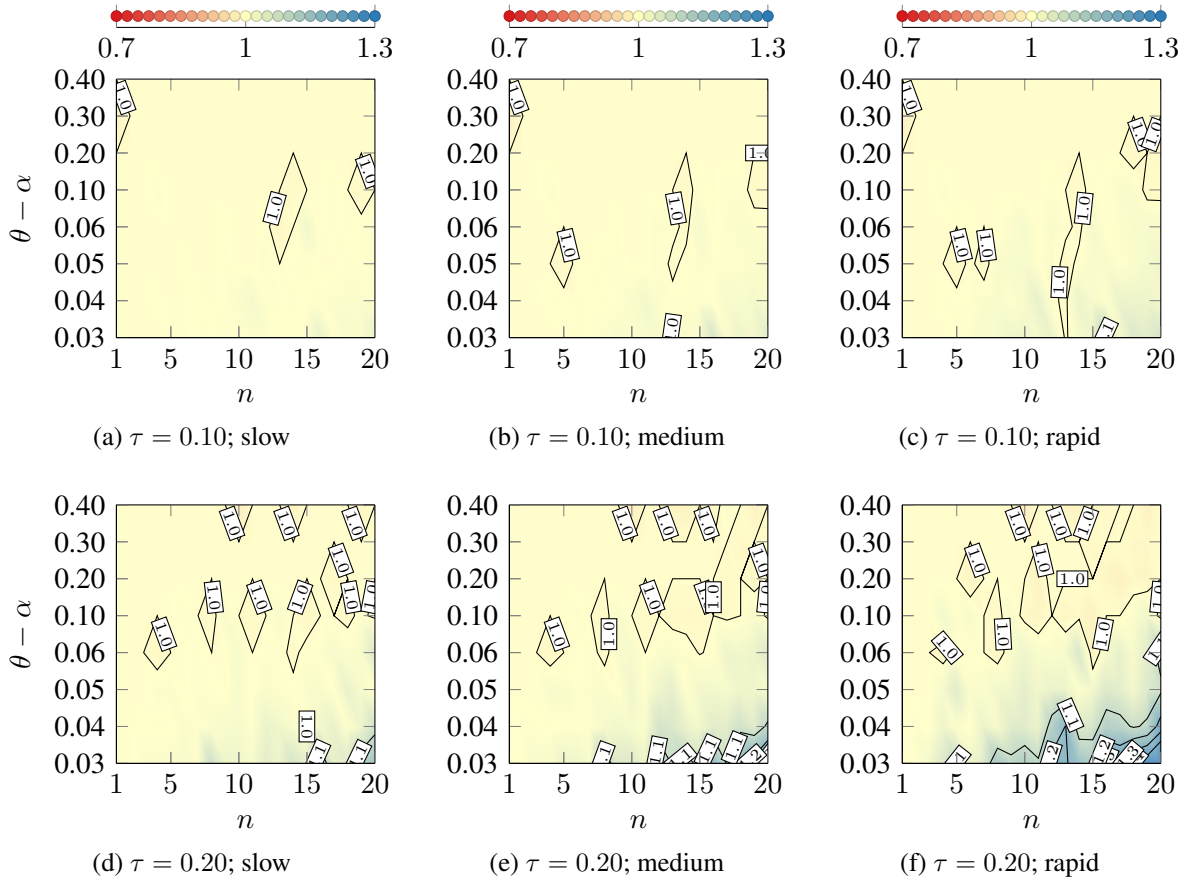

(a) $\tau = 0.10$; slow (b) $\tau = 0.10$; medium (c) $\tau = 0.10$; rapid

(d) $\tau = 0.20$; slow (e) $\tau = 0.20$; medium (f) $\tau = 0.20$; rapid

Figure 13: Efficiency of proposed ESDOF model ($CC_{p50}^{*,basecase}/CC_{p50}^{*}$) for a fixed stiffness quantification factor τ and different "speeds" of deterioration: non-deteriorating ESDOF system versus deteriorating ESDOF system

the prediction of the median collapse capacity is not affected by consideration of material deterioration, both for stiff and flexible frame structures. This result is desired because in this parameter domain material deterioration has no significant influence on the "exact" collapse prediction. Material deterioration has the largest impact on the median collapse capacity of high-rise flexible buildings with small negative stiffness ratio $\theta_i - \alpha$, i. e. $\tau = 0.20$, $\theta_i - \alpha = 0.03$ to 0.06, and $n = 10$ to 20. For this parameter set the proposed deteriorating ESDOF model should yield closer approximation of the collapse capacity than the non-deteriorating ESDOF model, which considers PDelta only. As it has already been discussed before, Figures 11d to 11f show that the proposed ESDOF model overestimates the collapse capacity of the MDOF system. Figures 13d to 13f illustrate that an ESDOF system without considering material deterioration would lead to a much larger overestimation of the median collapse capacity. For instance, in the worst case for a 20-story flexible building ($\tau = 0.20$) with $\theta_i - \alpha = 0.03$ the collapse capacity ratio $CC_{p50}^{*,basecase}/CC_{p50}^{*}$ is 1.63. Thus, it can be concluded that the proposed ESDOF system considering material deterioration improves the accuracy of simplified collapse prediction of PDelta vulnerable deterioration frame structures.

6 SUMMARY AND CONCLUSION

In this paper the influence of component deterioration on the collapse capacity of PDelta vulnerable frame structures has been quantified. The main objective has been to reveal and to validate the range of applicability of a proposed equivalent single-degree-of-freedom (ESDOF) system for simplified assessment of the global seismic collapse capacity. From the results of this study it can be concluded that component deterioration hardly reduces the median collapse capacity of highly PDelta vulnerable frame structures with a negative post-yield stiffness ratio between 0.10 and 0.40. Therefore, in those cases it is sufficient to use a non-deteriorating ESDOF constitutive model for a simplified collapse assessment. In general for low to moderate rise MDOF frame structures up to seven stories the collapse capacity predictions based on the proposed ESDOF model are reasonably accurate, independently of the significance of component deterioration. In high-rise frame structures with 10 to 20 stories, where PDelta leads to a small negative post-yield stiffness ratio in the range of 0.03 to 0.06, component deterioration has the largest effect on the median collapse capacity. For structures within this parameter range the proposed ESDOF system overestimates the median collapse capacity up to a factor of 2.12. This could be an indicator that the identified deterioration parameters of the ESDOF system are too large for flexible and high-rise structures. However, the collapse prediction using the proposed ESDOF model is much more accurate compared to a classical non-deteriorating one. For a non-deteriorating ESDOF model this factor increases to 3.5.

ACKNOWLEDGEMENT

This work was supported by the Austrian Ministry of Science BMWF as part of the UniInfrastrukturprogramm of the Focal Point Scientific Computing at the University of Innsbruck.

REFERENCES

[1] C. Adam, L.F. Ibarra, Seismic collapse assessment. *Earthquake Engineering Encyclopedia*. Accepted for publication, Springer Berlin Heidelberg. 2014.

[2] C. Adam, L.F. Ibarra, H. Krawinkler, Evaluation of P-delta effects in non-deteriorating MDOF structures from equivalent SDOF systems. *Proceedings of the 13th World Conference on Earthquake Engineering (13WCEE)*, Vancouver, B.C., Canada, Aug. 1-6, Paper No. 3407, 2004.

[3] C. Adam, C. Jäger, Seismic collapse capacity of basic inelastic structures vulnerable to the P-delta effect. *Earthquake Engineering & Structural Dynamics*, **41**, 775–793, 2012.

[4] C. Adam, C. Jäger, Simplified collapse capacity assessment of earthquake excited regular frame structures vulnerable to P-delta. *Engineering Structures*, **44**, 159–173, 2012.

[5] C. Adam, H. Krawinkler, Large displacement effects on seismically excited elastic-plastic frame structures. *Asian Journal of Civil Engineering (Building and Housing)*, **5**, 41–55, 2004.

[6] C. Adam, S. Tsantaki, L. Ibarra, D. Kampenhuber, Record-to-record vulnerability of the collapse capacity of multi-story frame structures vulnerable to P-Delta. *Proceedings of the Second European Conference on Earthquake Engineering and Seismology (2ECEES)*, Istanbul, Turkey, Aug. 24-29, Paper No. 132, 2014.

[7] C. Chintanapakdee, A. Jaiyong, Estimation of peak roof displacement of degrading structures. *Proceedings of the 15th World Conference on Earthquake Engineering (15WCEE)*, Lisboa, Portugal, Sept. 24-28, DVD–ROM paper 835, 2012.

[8] A.K. Chopra, *Dynamics of Structures. 3rd Edition*. Pearson Education. 2012.
[9] P. Fajfar, Structural analysis in earthquake engineering – a breakthrough of simplified non-linear methods. *Proceedings of the 12th European Conference on Earthquake Engineering (12ECEE)*, London, UK, Sept. 9-13, CD–ROM paper 843, 2002.
[10] C. Felippa, *Introduction to Aerospace Structures (ASEN 3112)*, Lecture notes, University of Colorado at Boulder. 2014.
[11] FEMA-P695, *Quantification of Building Seismic Performance Factors*. Federal Emergency Management Agency (FEMA), 2009.
[12] F. Graziotti, A. Penna, G. Magenens, Use of equivalent SDOF systems for the evaluation of displacement demand for masonry buildings. *Proceedings of the Vienna Congress on Recent Advances in Earthquake Engineering and Structural Dynamics 2013 (VEESD 2013)*, ed. by C. Adam, R. Heuer, W. Lenhardt, C. Schranz. Vienna, Austria, Aug. 28-30, Paper No. 347, 2013.
[13] L.F. Ibarra, H. Krawinkler, *Global collapse of frame structures under seismic excitations*. Report No. 152, The John A. Blume Earthquake Engineering Research Center, Department of Civil and Environmental Engineering, Stanford University, Stanford, CA., 2005.
[14] L.F. Ibarra, R.A. Medina, H. Krawinkler, Hysteretic models that incorporate strength and stiffness deterioration. *Earthquake Engineering & Structural Dynamics*, **34**, 1489–1511, 2005.
[15] C. Jäger, *The collapse capacity spectrum method. A methodology for rapid assessment of the collapse capacity of inelastic frame structures vulnerable to P-delta subjected to earthquake excitation (in German)*. PhD thesis, University of Innsbruck, 2012.
[16] D. Kampenhuber, C. Adam, Degradation parameter for equivalent SDOF systems obtained from cyclic pushover analysis and parameter optimisation. *Proceedings of the Second European Conference on Earthquake Engineering and Seismology (2ECEES)*, Istanbul, Turkey, Aug. 24-29, Paper No. 275, 2014.
[17] D. Kampenhuber, C. Adam, Vulnerability of collapse capacity spectra to material deterioration. *Proceedings of the Vienna Congress on Recent Advances in Earthquake Engineering and Structural Dynamics 2013 (VEESD 2013)*, ed. by C. Adam, R. Heuer, W. Lenhardt, C. Schranz. August 28-30. Vienna, Austria, Paper No. 424, 2013.
[18] D. Lignos, H. Krawinkler, Deterioration modeling of steel components in support of collapse prediction of steel moment frames under earthquake loading. *Journal of Structural Engineering*, **137**.11, 1291–1302, 2011.
[19] D. Lignos, H. Krawinkler, *Sidesway collapse of deteriorating structural systems under seismic excitations*. Report No. 177, The John A. Blume Earthquake Engineering Research Center, Department of Civil and Environmental Engineering, Stanford University, Stanford, CA., 2012.
[20] E. Limpert, W.A. Stahel, M. Abbt, Log-normal distributions across the sciences: keys and clues. *BioScience*, **51**, 341–352, 2001.
[21] G.A. MacRae, P-Δ effects on single-degree-of-freedom structures in earthquakes. *Earthquake spectra*, **10**, 539, 1994.
[22] R.A. Medina, H. Krawinkler, *Seismic demands for nondeteriorating frame structures and their dependence on ground motions*. Report No. 144, The John A. Blume Earthquake Engineering Research Center, Department of Civil and Environmental Engineering, Stanford University, Stanford, CA., 2003.
[23] N. Shome, C.A. Cornell, P. Bazzurro, J.E. Carballo, Earthquakes, records, and nonlinear responses. *Earthquake spectra*, **14**.3, 469–500, 1998.

[24] S. Tsantaki, *A contribution to the assessment of the seismic collapse capacity of basic structures vulnerable to the destabilizing effect of gravity loads*. PhD thesis, University of Innsbruck, 2014.

[25] D. Vamvatsikos, C.A. Cornell, Incremental dynamic analysis. *Earthquake Engineering & Structural Dynamics*, **31**, 491–514, 2002.